# Comparative Study of Experimentally Measured and Calculated Solar Radiations for Two Sites in Algeria

Bouazza Fekkak [1,*] , Mustapha Merzouk [2], Abdallah Kouzou [1,3,4] , Ralph Kennel [1],
Mohamed Abdelrahem [1,5,*] , Ahmed Zakane [6] and Mostefa Mohamed-Seghir [7]

1. Institute for Electrical Drive Systems and Power Electronics, Technical University of Munich (TUM), 80333 Munich, Germany; kouzouabdellah@ieee.org (A.K.); ralph.kennel@tum.de (R.K.)
2. Department of Renewable Energies, Faculty of Technology, Saad Dahlab University, Blida 09000, Algeria; mu.merzouk@gmail.com
3. Applied Automation and Industrial Diagnosis Laboratory (LAADI), Faculty of Science and Technology, Ziane Achour University of Djelfa, Djelfa 17000, Algeria
4. Electrical and Electronics Engineering Department, Nisantasi University, Istanbul 34398, Turkey
5. Department of Electrical Engineering, Assiut University, Assiut 71516, Egypt
6. National Higher School of Statistics and Applied Economics, Kolea 42000, Algeria; a.zakane@gmail.com
7. Department of Ship Automation, Gdynia Maritime University, 81-225 Gdynia, Poland; m.mohamed-seghir@we.umg.edu.pl
* Correspondence: fekkak@ieee.org (B.F.); Mohamed.abdelrahem@tum.de or Mohamed.abdelrahem@aun.edu.eg (M.A.)

**Abstract:** This paper presents a comparison study between the measured solar radiations on site and the calculated solar radiation based on the most theoretical models presented in the literature up to date. Indeed, for such purposes, this paper focusses on the analysis of the data of the measured solar radiation collected on two sites in Algeria such as Tlemcen ($34°52'58''$ N $01°19'00''$ W, elevation 842 m) and Senia ($35°39'$ N $0°38'$ W, elevation: 77 m). In order to check the accuracy of the proposed model, the experimental collected data of the solar radiation obtained from the existing radiometric stations installed at the two locations under investigation, are compared with the estimated or predicted solar radiations obtained from the Capderou and R.Sun models, where four days under clear skies are selected from different seasons to achieve this comparison. Second, the daily averages of the experimental global solar irradiation are compared to those predicted by Mefti model for both the sites. Finally, a validation is carried out based on the obtained experimental monthly global irradiations and with those estimated by Coppolino and Sivkov models. A relative difference is used in this case to judge the reliability and the accuracy of each model for both sites.

**Keywords:** solar radiation; Linke turbidity factor; clearness index; sunshine ratio; attenuation coefficient

## 1. Introduction

Nowadays, the large part of the world energy demand is ensured by conventional sources such as natural gas, oil, and coal. However, these sources are still expensive, exhaustible, and have finite reserves and they are considered as the major cause of the environmental degradation [1]. These drawbacks have urged all the actors of energy to look for alternative sources such as the new renewable energy sources to overcome at least the aforementioned disadvantages. Indeed, solar energy is one among these sources that are considered sustainable, environmentally friendly, and appendance all over the world without limitation. Therefore, the precise knowledge of solar radiation data of a specified location is very relevant for the rational exploitation of such energy source. Indeed, these data are essential for the design, the sizing, and the implementation of solar plants such as the photovoltaic systems (PV), which are expected to ensure the energy production to

fulfill the specific location energy demand requirements partly or totally depending on the demand schedules and the available amount of the solar energy [2].

The solar radiation calculation in a specific region is more or less accurate depending on the number of radiometric stations. These stations allow collecting onsite data that can be characterized depending on the mode of measurements such as the step time of data (month, day, and hour), the data nature (sunshine duration, solar radiation components and ground albedo, etc. ...). The need to the radiation data collection is a key factor for the sizing of PV systems as well as their adequacy to the concerned location. Whereas the accurate and reliable data are necessary at least for the economic aspect regarding the efficiency of solar energy conversion before the installation of a solar power plant in the concerned region [3].

Although, there is a network of solar measurement stations in in the whole world, their number is still limited and insufficient. Indeed, the solar radiations are measured only on limited number of sites around the world. On the other side, the real time radiation measurement can be achieved by special equipment, which requires a lot of material and instruments as well as their maintenance in order to ensure its reliable operation. Thus, the local meteorological stations whose budget is limited cannot meet such requirements [4]. For example, solar radiation measurement in Algeria is carried out by the National Meteorological Office (O.N.M). Through its network that is spread in the whole country, eighty-one (81) meteorological stations are dedicated to the measurement of the sunshine duration. Among these, only seven (07) stations "between 1970 and 1989" are used to ensure the measurement of the diffuse and global solar radiations received on a horizontal plane [5]. Indeed, since 2009, eight other automatic stations were installed in different regions to ensure the onsite measurements of the solar radiation components such as in Algiers airport, Senia, In Amenas, Ghardaïa, Annaba, Tamanrasset, Tlemcen and Constantin [5]. Furthermore, as long as the number of these stations is insufficient, various models are proposed to estimate the solar radiation potential on a local or regional scale. These models range from the most complex and sophisticated models to the simple models which are based on empirical formulation. Whereas the model choice depends on the data nature and the desired accuracy to be achieved. For example, for the estimation of the incident solar radiation, models are established based on some correlations form, which are related to the sites under consideration.

It is important to clarify that the design and sizing of energy system partially depend on the instantaneous values of meteorological variables measured on the ground for the concerned sites. However, these measurements can be accurate only for a specific location with limited area, which may present a major drawback in this case. To overcome such problem, the statistical models of the solar radiation based on hourly, daily, monthly, or even annual data are developed. These models are used in order to highlight the direct relationship between global and diffuse solar radiation. The first work which was carried out by Angstrom in 1924 [6–8], proposed a relation between the global radiation on a horizontal surface and sunshine fraction. After some year, exactly in 1960, Liu-Jordan proposed a relation between the diffuse fraction and the clearness index [9]. Considering that, these two proposed correlations were original discovers in this field at that time and which were developed to be applied for daily intervals, they were used for the calculation of the diffuse fraction as a function of the clearness index $k_t$ and as a function of the sunshine fraction σ for hourly intervals. Indeed, after these two proposals several authors such as Rietveld [10], Glover and McCulloch [11], Hussain 1982 [12], Angström-Prescott [13], Orgill and Hollands [14], and others have established models to estimate global solar radiation based on some specific important meteorological parameters such as the temperature, the humidity, the cloudiness, and the most used among researcher and experimentally the sunshine duration.

In this study, a new approach is proposed which is built based on the collected onsite data for one year. Indeed, this model is compared with five chosen models among the previously existing models. Where, for the radiation estimation under clear skies, the

Capderou [2] and R.Sun [15] models are used. For the estimation of the monthly average global irradiation, the weather model of Coppolino is used [16]. For the estimation of the daily average global irradiation, Coppolino model with Sivkov model is used [17,18]. Wherein, for the estimation of the monthly average daily global radiation, Mefti model is used [19]. It is important to clarify that a relative error is evaluated in this case to judge the reliability of each model in both sites.

The second main contribution in this paper is concerning the estimation of the Linke turbidity Factor $T_L^*$ under clear skies. The main proposed idea is to estimate the Linke turbidity factor based on combining the well-known two models such as the Capderou model and R.Sun model.

The present paper is structured on an introduction and five sections. The second section focusses on the presentation of the main parameters of the investigated models, which are taken into consideration in this study. The third section presents a model proposed by the authors. The fourth section is mainly dedicated to the detailed presentation of the models presented in the literature up to date. In the fifth section the data of the radiometric characterization of two studied regions such as Senia and Tlemcen are presented. The last section is reserved to the comparison of the real data collected onsite and the simulation results of proposed approach in the main aim of its validation. The paper ends with a conclusion.

## 2. The Principle of the Proposed Model

The climatic parameter of sunshine duration is the most suitable parameters among the other aforementioned parameters which is used for the experimental measurements because it is the most available and can be easily measured. Thus, it can be considered as an inexpensive factor for solar radiation evaluations [20].

Indeed, the meteorological stations all over the world, were used for the measurement of the sunshine duration for many years. Whereas, since few years, attempts were carried out to estimate the global radiation received on a horizontal plane from the sunshine fraction. The resulting correlations from these attempts allow reconstructing solar radiation in a specific location where only sunshine duration is known. However, these proposed correlations generally have an important limitation that they allow reconstituting only a single component of the radiation. Thus, the model proposed in this paper will allow overcoming this limitation by reconstituting the global and the diffuse radiation components at the same time based on the knowledge of the sunshine fraction and the clearness index.

The sunshine fraction and clearness index are deducted from measurable parameters such as sunshine duration $S$ and daily global solar irradiation $H_g$, and the calculable parameters such as the daily extraterrestrial solar irradiation $H_0$ and the theoretical duration of the day $S_0$. This proposed concept allows constructing the ratio of the daily diffuse solar irradiation to the daily solar global irradiation $\frac{H_d}{H_g}$ based on two correlations. The first one is function of the sunshine fraction $\sigma$ and the second one is function of clearness index $k_t$, which are expressed as follows:

$$\begin{cases} \frac{H_d}{H_g} = a + b\sigma \\ \frac{H_d}{H_g} = a_1 + b_1 k_t \end{cases} \tag{1}$$

where: $a, b, a_1, b_1$ are the parameters of the proposed linear model, which can be determined based on the measured data from sites of Tlemcen and Senia. It is worthy to clarify here that many models have been tested along the work presented in this paper such as the polynomial regression with different orders and even a logarithmic model. However, based on different obtained results, it was concluded that the linear model was the best suitable model for the case of the study presented in this paper.

For the present study, the two correlations presented in Equation (1) are established based on the metrological data obtained from the sites of Senia and Tlemcen, during the

year of 2006. This was only possible after careful examination and sorting of all the values of the parameters provided by the National Office of Meteorology (NOM).

The monthly average global irradiation can be calculated based on the daily global irradiation which can be obtained from the proposed linear model presented in Equation (1) as follows:

$$\begin{cases} \frac{H_{di}}{H_{gi}} = a + b\sigma_i \\ \frac{H_{di}}{H_{gi}} = a_1 + b_1\,k_{t_i} \end{cases} \tag{2}$$

$a$, $b$, $a_1$, $b_1$ are the regression coefficients of the proposed linear models, $i$ is the number of the day in the month.

Based on the available data, these coefficient have been determined for each month for both the sites of Senia and Tlemcen as presented in Tables 1 and 2 respectively.

On the other side, the values of the daily clearness index $k_{ti}$ and the daily global solar irradiation $H_{gi}$ corresponding to day $i$ of the month can be deduced from Equation (2) as follows:

$$\begin{cases} k_{t_i} = \frac{H_{gi}}{H_{csi}} = \frac{a-a_1+b\sigma_i}{b_1} \\ H_{gi} = H_{sci}\frac{a-a_1+b\sigma_i}{b_1} \end{cases} \tag{3}$$

$H_{sci}$ is the daily global irradiation at the top of the atmosphere.

It is worthy to clarify that for the proposed linear model, the monthly average of the global irradiation is calculated and which can be expressed as:

$$\overline{H}_{gj} = \frac{a_j - a_{1j} + b_j\overline{\sigma}_j}{b_{1j}}\overline{H}_{csj} \tag{4}$$

$\overline{H}_{gi}$, $\overline{H}_{gi}$, $\overline{k}_{tj}$, and $\overline{\sigma}_i$ are the monthly average values of the month $j$ in the year.

**Table 1.** Regression coefficients of the fit by the relation 1 and 2: SENIA.

| | | $\dfrac{\overline{H}_{dj}}{\overline{H}_{gj}} = a_j + b_j\overline{\sigma}_j$ | | | | $\dfrac{\overline{H}_{dj}}{\overline{H}_{gj}} = a_{1j} + b_{1j}\,\overline{k}_{t_j}$ | | |
|---|---|---|---|---|---|---|---|---|
| **Month** | $b_j$ | $a_j$ | $R^2$ | **RMSE** | $b_{1j}$ | $a_{1j}$ | $R^2$ | **RMSE** |
| **January** | −0.8711 | 0.9009 | 0.9149 | 0.0741 | −1.4285 | 1.2373 | 0.8698 | 0.0916 |
| **February** | −0.6610 | 0.8740 | 0.7563 | 0.1150 | −1.1398 | 1.1182 | 0.8760 | 0.0820 |
| **March** | −0.8708 | 0.9209 | 0.9377 | 0.0535 | −1.2194 | 1.1071 | 0.8941 | 0.0696 |
| **April** | −0.6582 | 0.8469 | 0.7891 | 0.0816 | −1.0257 | 1.0353 | 0.7409 | 0.0902 |
| **May** | −0.4654 | 0.8236 | 0.5485 | 0.1319 | −0.8992 | 1.0019 | 0.7023 | 0.1076 |
| **June** | −0.3928 | 0.8421 | 0.2657 | 0.1903 | −1.0962 | 1.1015 | 0.8250 | 0.0929 |
| **July** | −0.1272 | 0.4324 | 0.0595 | 0.0939 | −0.1094 | 0.4093 | 0.0224 | 0.0958 |
| **August** | −0.4274 | 0.9171 | 0.3012 | 0.1246 | −1.6606 | 1.0743 | 0.6584 | 0.0871 |
| **September** | −0.6342 | 0.7925 | 0.7746 | 0.0892 | −0.7731 | 0.8320 | 0.4171 | 0.1434 |
| **October** | −0.7996 | 1.0177 | 0.4918 | 0.1669 | −1.3770 | 1.2564 | 0.6943 | 0.1298 |
| **November** | −0.6278 | 0.8859 | 0.7114 | 0.1207 | −1.3941 | 1.3018 | 0.7706 | 0.1075 |
| **December** | −0.7568 | 0.9003 | 0.8369 | 0.1077 | −1.3762 | 1.2171 | 0.7999 | 0.1193 |

R is the correlation factor and RMSE is the root mean square error.

**Table 2.** Regression coefficients of the fit by the relation 1 and 2: Tlemcen.

| Month | $\dfrac{\overline{\overline{H_{dj}}}}{\overline{H_{gj}}}=a_j + b_j \overline{\sigma_j}$ | | | | $\dfrac{\overline{\overline{H_{dj}}}}{\overline{H_{gj}}}=a_{1j} + b_{1j}\,\overline{k_{t_j}}$ | | | |
|---|---|---|---|---|---|---|---|---|
| | $b_j$ | $a_j$ | $R^2$ | RMSE | $b_{1j}$ | $a_{1j}$ | $R^2$ | RMSE |
| January | −0.8302 | 0.9114 | 0.9122 | 0.0803 | −0.9663 | 1.0971 | 0.9177 | 0.0777 |
| February | −0.8217 | 0.9240 | 0.8269 | 0.1056 | −0.9336 | 1.0556 | 0.7998 | 0.1135 |
| March | −0.8065 | 0.8574 | 0.7957 | 0.0828 | −0.7203 | 0.8720 | 0.5971 | 0.1163 |
| April | −0.6337 | 0.8338 | 0.7536 | 0.0996 | −0.7637 | 0.9755 | 0.8367 | 0.0811 |
| May | −0.6105 | 0.8220 | 0.8338 | 0.0771 | −0.7097 | 0.9516 | 0.8688 | 0.0685 |
| June | −0.7927 | 0.9516 | 0.8220 | 0.0829 | −0.9871 | 1.1492 | 0.9282 | 0.0527 |
| July | −0.4887 | 0.7073 | 0.4170 | 0.0654 | −0.9829 | 1.1429 | 0.7544 | 0.0425 |
| August | −0.6820 | 0.8205 | 0.4996 | 0.0549 | −1.0703 | 1.1808 | 0.7406 | 0.0395 |
| September | −0.6698 | 0.7980 | 0.6193 | 0.0934 | −0.8924 | 1.0202 | 0.7717 | 0.0724 |
| October | −0.7527 | 0.8698 | 0.8040 | 0.0887 | −1.0151 | 1.1489 | 0.9004 | 0.0635 |
| November | −0.8734 | 0.9638 | 0.8707 | 0.0924 | −1.0704 | 1.1805 | 0.8700 | 0.0926 |
| December | −0.8205 | 0.9406 | 0.8938 | 0.0871 | −1.0378 | 1.1413 | 0.8874 | 0.0898 |

R is the correlation factor and RMSE is the root mean square error.

## 3. Main Parameters of the Studied Models

### 3.1. Linke Turbidity Factor

The atmospheric turbidity expresses the attenuation of the solar radiation that reaches the earth's surface under cloudless sky and describes the optical thickness of the atmosphere. In 1922 Linke introduced the idea of the turbidity factor, eventually named the Linke turbidity factor [21]. It is defined as the number of clean and dry atmospheres that would be necessary to produce the same attenuation of the extra-terrestrial solar radiation that is produced by the real atmosphere. It is obtained from pyrheliometre measurements of direct solar radiation. It is expressed as follows:

$$T_L{}^* = \frac{k}{k_0} \tag{5}$$

where $k$ is the real attenuation coefficient and $k_0$ is the attenuation coefficient in pure atmosphere. Kasten has defined this factor as [22]:

$$k_0 = \frac{1}{9.4 + 0.9m} \tag{6}$$

$m$ is the air mass coefficient.

Iqbal et al. have modified Equation (6), the new attenuation coefficient in pure atmosphere is expressed as follows [23]:

$$k_0 = \frac{1}{9.4 + 0.8m - 5exp\left(-\frac{m}{2}\right)} \tag{7}$$

Indeed, the Linke turbidity factor for total radiation is explained physically by the sum of the attenuation effects integrated across the sun spectrum resulting from the scattering and absorption of sunlight in the atmosphere in addition to the effect of clouds.

In this context, several complex models have been developed for the estimation of the Linke turbidity factor, which are based on different separated attenuation causes. One of this models is the Dogniaux-Brichambaut model [15]. Once the Linke turbidity factor

is estimated, the direct solar radiation on a horizontal plane at the earth surface can be calculated as follows [23]:

$$I_b = I_0 C_T exp\left(-\frac{(T_L{}^*)}{0.9 + \frac{9.4}{0.89^z}.sin(h)}\right)sin(h) \tag{8}$$

$z$ is the altitude of the concerned location measured in meter, $h$ is the sun elevation (altitude) angle, $I_0$ is the energy flux density at 1 AU (the mean earth/sun distance of 149,597,890 km), also known as solar constant and it is equal to 1367 W·m$^{-2}$, and $C_T$ is the correction coefficient of the earth–sun distance. It expressed as follows [24]:

$$C_T = 1 + 0.034 \cos(N - 2) \tag{9}$$

$N$ is the day number of the year (1 correspond to the first of January).

### 3.2. Solar Declination Angle

The solar declination angle denoted by $\delta$ (degrees) is the angle between a ray of the sun and the equatorial plane. It varies seasonally due to the rotation of the earth around the sun and the tilt of the earth on its rotation axis. It varies from $-23.45°$ in winter solstice to $+23.45°$ in summer solstice. In vernal and autumnal equinoxes, it is equal to zero degree. The solar declination angle is defined by Copper in 1969 as follows [25]:

$$\delta = 23.45 \, sin\left(\frac{360}{365}(284 + N)\right) \tag{10}$$

$N$ is the day number of the year (1 correspond to the first of January).

### 3.3. Clearness Index

It is obvious that the incoming solar radiation is transmitted through the earth atmosphere before it strikes the earth surface. Therefore, the solar irradiation which reaches the surface of the external layer of the atmosphere $H_0$ is attenuated by different atmosphere layers and components before it strikes the earth surface by the attenuated solar irradiation components $H_g$. The clearness index $K_t$ is a dimensionless number, which ranges between zero and one and measures the attenuation degree of extraterrestrial solar irradiation $H_0$ along its path from the external surface of the atmosphere to the earth surface. The monthly clearness index is defined as follows [9,26]:

$$K_t = \frac{H_g}{H_0} \tag{11}$$

$H_g$ is the predicted monthly averaged daily global solar irradiation on a horizontal surface (KWh·m$^{-2}$ day$^{-1}$), $H_0$ is the solar irradiation at the top of the atmosphere received at a horizontal surface on the external side of the atmosphere (KWh·m$^{-2}$ day$^{-1}$).

The monthly averaged clearness index $K_t$ varies by location and by season. It is generally between 0.3 for rainy regions or rainy seasons and 0.8 for dry and sunny climates or dry and sunny seasons. It is worthy to note that it is possible to define the daily and hourly averaged clearness index as well.

### 3.4. Sunshine Duration (S)

The sunshine duration $S$ is defined as the length of time, in particular within a day, during which the earth surface receives solar radiation. In the permanent absence of clouds, the sunshine duration is practically equal to the duration of the day from the sunrise to

the sunset, it is also called astronomical or theoretical duration of the day. The maximum sunshine duration (monthly averaged day length) $S_0$, is defined as [27]:

$$S_0 = \frac{2}{15}\omega_0 \tag{12}$$

$\omega_0$ is the hour angle at sunset measured in degree.

### 3.5. Sunshine Ratio (σ)

During the day, which is characterized by its specific duration, the earth surface receives maximum solar radiation under clear skies. However, effective duration of ordinary day sunshine is less than the day specific duration due to the climatic changes in the atmosphere. To quantify this effect, the sunshine ratio $\sigma$ is introduced, and defined as follows [28]:

$$\sigma = \frac{S}{S_0} \tag{13}$$

## 4. Main Models Presentation

### 4.1. Estimation of Solar Radiation under Clear Skies

In the case of a clear day, the fast and easy evaluation method of the power received on the earth surface within a horizontal plane can be obtained based on several simplified models, which are proposed in several previous works. In this paper, these main models are presented.

### 4.1.1. Semi Empirical Model of Perrin de Brichambaut

This model is presented by the following formulas [23]:

$$I_g = I_b + I_d \tag{14}$$

$$I_b = A\sin(h)exp\left\{-[C\,sin(h+2)]^{-1}\right\} \tag{15}$$

$$I_d = B(sin(h))^{0.4} \tag{16}$$

Based on Equation (14), it is clear that the global solar radiation $I_g$ presents the sum of direct solar radiation component $I_b$ and the diffuse solar radiations component $I_d$, it can also be calculated directly as follows:

$$I_g = D(sinh)^E \tag{17}$$

$h$ presents the sun elevation angle. The coefficients A, B, C, D, and E, which depend on the sky clearness are presented in Table 3. [23].

**Table 3.** Coefficients given by Perrin de Brichambaut.

| Sky Clearness | A(W/m$^2$) | B(W/m$^2$) | C(W/m$^2$) | D(W/m$^2$) | E |
|---|---|---|---|---|---|
| Dark blue sky | 1300 | 87 | 6 | 1150 | 1.15 |
| Clear blue sky | 1230 | 125 | 4 | 1080 | 1.22 |

The experience has shown that the application of this model leads to an overestimation of the solar radiation [2].

### 4.1.2. Capderou Model 1987

The Capderou model, which is based on the Brichambaut model, uses the atmospheric turbidity factor for the calculation of the direct and diffuse components of the solar radiation received on a horizontal plane [2]. The absorption and diffusion caused by the constituents of the atmosphere can be expressed as function of Linke turbidity factors. In this model

the Linke turbidity factors $T_L^*$ under clear skies are composed of three components as follows [24,29]:

$$T_L^* = T_0 + T_1 + T_2 \tag{18}$$

$T_1$ is the turbidity factor due to the molecular diffusion, $T_2$ is the turbidity factor relative to the aerosol diffusion and $T_0$ is the turbidity factor related to gas absorption ($O_2$, $CO_2$, $O_3$) including atmosphere, ozone, and water vapor, it is defined as:

$$T_0 = \frac{9.4 + 0.9m_a}{m_a}\alpha_{aw} \tag{19}$$

$\alpha_{aw}$ is the attenuation coefficient which presents the effect of the water vapor absorption. $m_a$ is the relative optical dry air mass, it has no unit and is defined as follows [19]:

$$m_a = \frac{p}{p_0}\frac{1}{\sin(h) + 0.15(h + 3.885)^{-1.253}} \tag{20}$$

where $\frac{p}{p_0}$ can be expressed calculated by the following expression [30]:

$$\frac{p}{p_0} = exp\left(-\frac{z}{z_h}\right) \tag{21}$$

$z$ is the site elevation and $z_h$ is the scale height of the Rayleigh atmosphere near the earth surface which is equal to 8434.5 m.

The modeling of these three components of the Linke turbidity factors $T_L^*$ as a function of only geo-astronomical parameters has allowed Brichambaut to propose the following expression [2,24]:

$$T_0 = 2.4 - 0.9sin(\varphi) + 0.1(2 + sin(\varphi))A_{ws} - 0.2z - (1.22 + 0.14\ A_{ws})(1 - sin(h)) \tag{22}$$

$$T_1 = (0.89)^z \tag{23}$$

$$T_2 = (0.9 + 0.4\ A_{ws})(0.63)^z \tag{24}$$

$$A_{ws} = sin\left\{\left(\frac{360}{365}\right)(N - 121)\right\} \tag{25}$$

$A_{ws}$ is a sinusoidal function which reflects the winter-summer alternation, $N$ is the number of the day in the year, $\varphi$ is the latitude angle (in degrees), $z$ is the altitude of the location under study.

Based on the estimation of the Linke turbidity factors $T_L^*$, the direct solar radiation obtained on a horizontal plane attenuated by cloudless atmosphere can be calculated by the expression proposed by Capderou as follows [2,15]:

$$I_b(h,\ T_{Lk}) = I_0 sin(h) exp\{-0.8662\ T_{Lk}m_a\delta_R(m_a)\} \tag{26}$$

$h$ is the incidence angle or the sun elevation, $m_a$ is the relative optical air mass (AM2), $T_{Lk}$ is the Linke turbidity factor. $I_0$ is the extraterrestrial solar radiation normal to horizontal plane. $\delta_R(m)$ is the Rayleigh integral optical thickness defined by Kasten [31].

The diffuse solar radiation obtained on a horizontal plane also depends on the diffusive turbidity factor $T'_{LD}$, this factor is defined as follows:

$$T'_{LD} = T_1 + T_2 = T_L^* - T_0 \tag{27}$$

The diffuse solar radiation is then defined as:

$$I_d = I_0 exp(-1 + 1.06log(sin(h)) + a - \sqrt{b^2 + a^2} \tag{28}$$

with:

$$\begin{cases} b = log(T_L^* - T_0) - 2.80 + 1.02(1 - sin(h))^2 \\ a = 1.1 \end{cases} \qquad (29)$$

Finally, the global solar radiation can be calculated in the similar way which was used in the empirical Perrin de Brichambaut model presented in Equation (14):

$$I_g = I_b + I_d \qquad (30)$$

The atmospheric cloudiness estimation model was presented by Kasten in 1996 [31,32]. Where, the Linke turbidity factor was defined based on the direct radiation received on a normal plane under clear skies $I_d$, the sun constant (1367 W/m$^2$) or the extraterrestrial solar radiation $I_0$, the Rayleigh integral optical thickness $\delta_R$, the atmospheric air mass $m_a$ which depends on the sun elevation angle $h$ and local air pressure $P$, the earth's orbit eccentricity correction factor $\varepsilon$ that can be calculated with Spencer's, as follows [32]:

$$T_L = -\frac{1}{\delta_R m_a} log\left(\frac{I_d}{I_0 \varepsilon}\right) \qquad (31)$$

$$1/\delta_R = 6.6296 + 1.7513 m_a - 0.1202 m_a^2 + 0.0065 m_a^3 - 0.00013 m_a^4 \qquad (32)$$

$$m_a = \frac{P}{101,325}\left[sin(h) + 0.15(h + 3.885)^{-1.253}\right]^{-1} \qquad (33)$$

The research of Gama et al. cited in [18] showed that the application of this model in Algeria led to an overestimation of the solar radiation.

### 4.1.3. R.Sun Model

In the model proposed by R.Sun in [19], the incident global solar radiation on a horizontal plane $I_g(h, T_L)$ under clear skies (W/m$^2$), is divided into two components: the direct solar radiation $I_b(h, T_L)$ (also named beam horizontal solar radiation) and the diffuse radiation $I_d(h, T_L)$. Where, each component can be calculated separately. The expression of the direct solar radiation incident on the horizontal plane under a clear sky, which was proposed by Capederou in (26), is combined with the R.Sun model. The diffuse solar radiation, received on a horizontal surface under clear skies $I_d$ (also named diffuse horizontal solar radiation), crosses the clouds and starts diffusing in all directions along its path passing through the atmosphere before reaching the earth surface, thus it depends on the Linke turbidity factor. The formula cited in [33] is used for the diffuse solar radiation calculation, with a slight correction factor. Indeed, the relative length of the optical path varies with the altitude $z$ of the measuring station above sea level. Therefore, a correction is applied to the turbidity factor which is the ratio of the mean atmospheric pressure ($p$) at the altitude of the site to the mean atmospheric pressure at sea level ($p_0$). This correction is particularly important in mountainous areas. It was adopted in 2004 by the new Europe Solar Atlas (ESRA) [19] and was taken into account in the 2007 in the MeteoNorm V6 [34].

The corrected turbidity factor is expressed as:

$$T_{Lc} = \left(\frac{p}{p_0}\right) T_L \qquad (34)$$

The diffuse solar radiation expression is then defined as follows:

$$I_d(h, T_{Lc}) = I_0 T_{rd}(T_{Lc}(h)) F_d(h, T_{Lc}(h)) \qquad (35)$$

$T_{rd}(T_{Lc}(h))$ is the diffuse transmittance function. It depends solely on the corrected turbidity factor $T_{Lc}(h)$, it varies between 0 and 0.3. It can be expressed as follows:

$$T_{rd}(T_{Lc}(h)) = -(1.5843)10^{-2} + (3.05430)10^{-2} T_{Lc}(h) + (3.797)10^{-4} T_{Lc}^2(h) \qquad (36)$$

$F_d(h, T_{Lc}(h))$ is the diffuse angular function. It depends on the sun elevation ($h$) and the corrected turbidity factor $T_{Lc}(h)$. It is defined by the following expression:

$$F_d(h, T_{Lc}) = A_0(T_{Lc}(h)) + A_1(T_{Lc}(h))sin(h) + A_2(T_{Lc}(h))[sin(h)]^2 \tag{37}$$

$A_0$, $A_1$, and $A_2$ are coefficients depending only on the corrected turbidity $T_{Lc}(h)$, which are defined as follows [21]:

$$\begin{cases} A_0 = (2.6463)10^{-1} - (6.1581)10^{-2}T_{Lc}(h) + (3.1408)10^{-3}T_{Lc}^2(h) \\ A_1 = 2.0402 + (1.8945)10^{-2}T_L(h) - (1.1161)10^{-3}T_L^2(h) \\ A_2 = -1.3025 + (3.9231)10^{-2}T_{Lc}(h) + (8.5079)10^{-3}T_{Lc}^2(h) \end{cases} \tag{38}$$

It was found, that $A_0$ leads to negative values if $T_L(h = AM2) > 6$. Hence, it was proposed to add a constraint to avoid such situation and to ensure acceptable values at sunrise and sunset. This constraint is defined as follows:

$$\text{if } A_0 T_{rd}(h) < 2.10^{-3} \text{ then } A_0 = 2.10^{-3}/T_{rd}(h) \tag{39}$$

This model is currently the most used for the different solar systems sizing codes such as PVGIS.

### 4.1.4. Full Perrin de Brichambaut Model

This model is valid for a Linke turbidity factor $T < 6$ and a latitude less than $60°$ (in absolute value), $T$ can be calculated based on the empirical formulation of Dogniaux [17,18]. This model is defined as follows [2,15]:

$$\begin{cases} \frac{H_{gc}}{H_0} = (0.91 - 0.15logT)cos^{0.13\sqrt{T^*}}(\varphi - \delta) \\ \frac{H_{dc}}{H_0} = 0.07(T - 1)cos^{-0.7}(\varphi - \delta) \\ \frac{H_{bc}}{H_0} = exp\frac{-T^*}{7.2\, cos^{0.75}(\varphi-\delta)} \end{cases} \tag{40}$$

$H_{gc}$ is the global daily solar irradiation under clear skies, $H_0$ is the daily extraterrestrial solar irradiation, $H_{dc}$ is the diffuse daily solar irradiation under clear skies. $H_{bc}$ is the direct daily solar irradiation under clear skies, $T^*$ is the turbidity factor under clear skies.

### 4.2. Estimation of the Solar Radiation under Variable Sky Clearness

Under the case of variable sky clearness, the established relationships estimate the mean solar irradiation as a function of the sunshine fraction or of the clearness index. These obtained daily solar irradiations on the concerned days, which are affected by the variable sky clearness, are summarized in Table 4, and they are compared to the mean monthly value $\overline{sin\, h}$ which is expressed as follows [2]:

$$\overline{sin\, h} = cos\varphi\, cos\delta\, \frac{sin\,\omega_s - cos\omega_s}{\omega_s} \tag{41}$$

$\omega_s$ is the sunrise hour angle.

The representative days for each month are given in the following table:

**Table 4.** Data of the respective days for each month.

| Month | Jan | Feb | Mar | Apr | May | Jun | Jul | Aug | Sep | Oct | Nov | Dec |
|---|---|---|---|---|---|---|---|---|---|---|---|---|
| **Day in Month** | 17 | 16 | 16 | 15 | 15 | 11 | 17 | 16 | 15 | 15 | 14 | 10 |
| **Day in Year** | 17 | 47 | 75 | 105 | 135 | 162 | 198 | 228 | 258 | 288 | 318 | 344 |

### 4.2.1. Meteorological Models

The meteorological models use linear relationships and allow transforming the data measured at the ground onsite (sunshine, temperature, etc.,) into global flux of solar radiation. These models have the advantage of being applied to any sky state.

Estimation of Monthly Averaged Daily Global Solar Irradiation: Coppolino Model 1989

In 1989, Coppolino proposed a very simple model, which allowed the prediction of the monthly averaged daily global solar irradiation at any location in Italy. Indeed, for achieving this prediction he used only the information of two parameters such as the sunshine duration S (hours) and the altitude of the sun at noon in the middle of each month (the 15th day of the month). This model is defined as follows [16]:

$$G = 7.8 \, S^{0.5}(sin(h_m))^{1.15} \tag{42}$$

$G$ is the monthly average daily global solar radiation (MJ/m$^2$/day), $S$ is the monthly averaged daily sunshine duration of the 15th day of the month (Hours), and $h_m$ is the altitude or elevation angle of the sun at noon on the 15th day of the month (degrees).

Estimation of the Monthly Global Solar Irradiation: SivKov Model 1964

In 1964, Sivkov proposed an empirical model for the estimation of the monthly global solar irradiation at latitudes 35° to 65°, which depend only on monthly sunshine duration, and the altitude of the location. The Sivkov model is expressed as follows [18]:

$$H_g = 4.9(n_m)^{1.31} + 10,500(sin(h_m))^{2.1} \tag{43}$$

$H_g$ is the monthly global irradiation (cal/cm$^2$) and $n_m$ is the monthly sunshine hours (hour).

## 5. Experimental Radiometric Characterization of Senia and Tlemcen

Many works were developed in order to find the relationship between the diffuse and global solar irradiations and the meteorological measured parameters as was described in detail in the last section. Based on the aforementioned studies, it can be concluded that in order to obtain an accurate model for the estimation of the three components of the solar irradiation, it is mandatory to perform a deep study of the impact of the more influencing parameters on these three components such as the sunshine duration and the clearness index. Furthermore, to ensure the conception of an accurate model, it is required to have more reliable and precise measurements of daily, monthly, and yearly solar irradiations for both sites of Senia and Tlemcen.

### 5.1. Study of Daily Sunshine Data

Due to the large area of Algeria, the sunshine duration $S$ is different from one region to another. Indeed, it is in the center and south of Algeria greater that the littoral band. Table 5 presents the annual sunshine duration for the two sites investigated in this paper such as Senia and Tlemcen.

**Table 5.** Annual sunshine duration.

| Site | Senia | Tlemcen |
|---|---|---|
| Duration (In Hours) | 2233.5 | 3104.4 |

### 5.1.1. Evolution of the Sunshine Daily Sequences

On a daily scale and based on real data collected onsite during one year, the sunshine duration in both the studied sites of Tlemcen and Senia, are characterized by high fluctuations as it can be clearly seen in the blue curves of Figure 1a,b. Whereas, the red curves present the maximum theoretical values of the sunshine under clear sky.
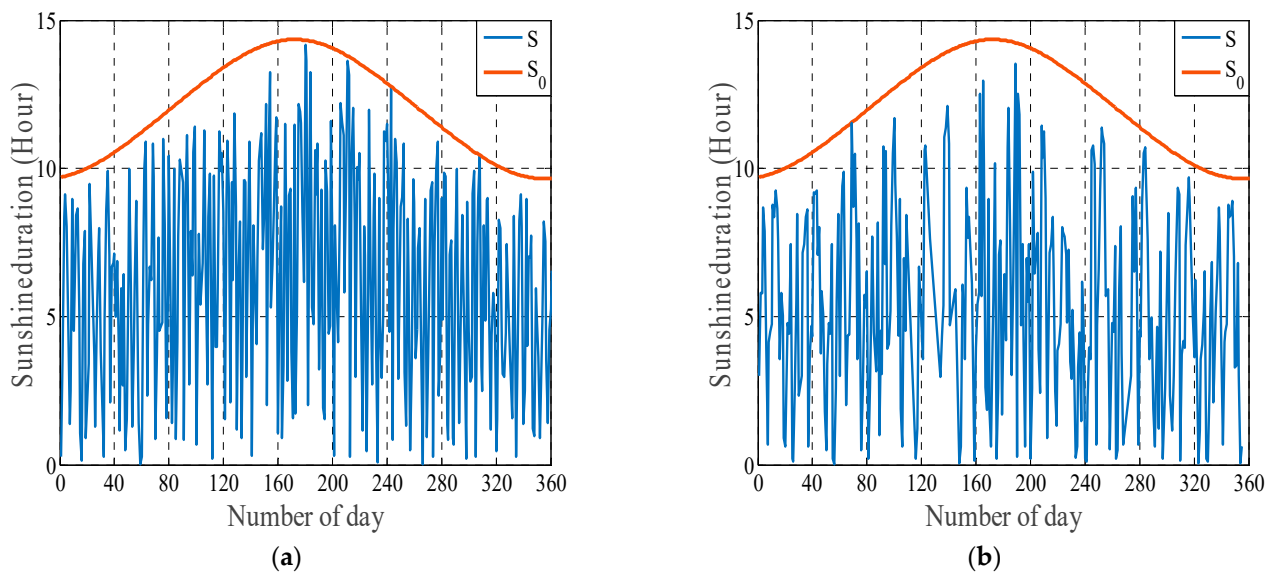
**Figure 1.** The daily variations of the maximum (theoretical) and the measured sunshine. (**a**) Curves for Tlemcen site; (**b**) Curves for Senia site.

### 5.1.2. Analysis of the Monthly Average Sunshine

The monthly sunshine duration averages constitute an important database for the study of the solar potential at studied sites. Figure 2a,b shows the measured on-site monthly averages of the sunshine duration variations $S$ in green color, and the theoretical maximum monthly averages sunshine duration $S_o$ under clear sky in red for the both sites under investigation such as Tlemcen and Senia respectively.
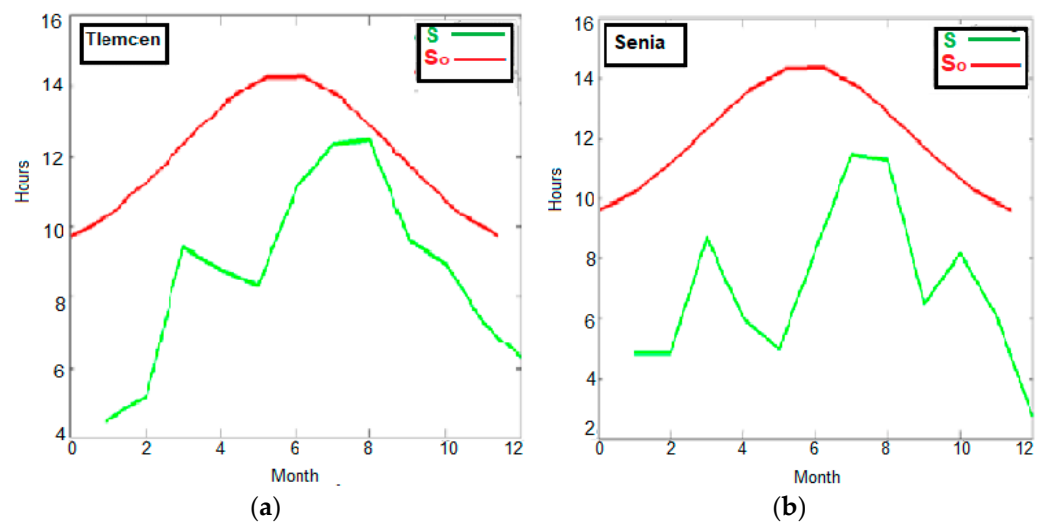


**Figure 2.** Monthly averages curves of measured and theoretical sunshine durations. (**a**) Curves for Tlemcen site; (**b**) Curves for Senia site.

Note that for Tlemcen, the sunshine duration S takes the same shape as the theoretical sunshine duration $S_0$ with difference of scale, except the months from March to May where S evolves inversely with $S_0$. The sunshine duration is high in summer (June, July, August) reaching 12 h, and low in winter between 4 and 5 h (December, January and February). For Senia, the sunshine duration $S$ changes much more than the theoretical sunshine duration $S_0$.

5.1.3. Histograms of Monthly Sunshine for Both Sites

Figure 3 shows the distributions of monthly averaged sunshine duration for both sites. It can be clearly noted that the distribution for Tlemcen is good except for the months of April and May. Contrary to the case of the site of Senia which is often characterized by cloudy days and therefore the distribution is not so adequate.
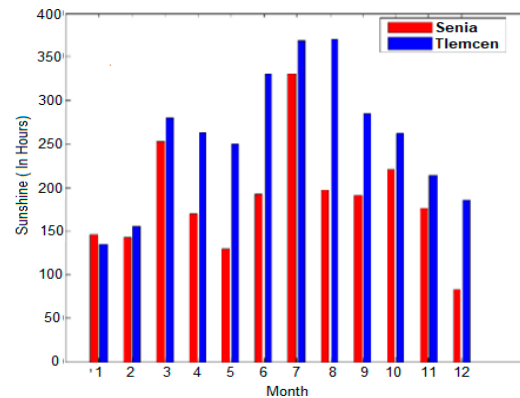


**Figure 3.** Distribution of Monthly sunshine durations for Tlemcen and Senia.

*5.2. Distribution of the Daily Clearness Index*

The daily clearness index $K_{dt}$, which is the ratio of the global solar irradiation received on ground ($H_g$) to the solar irradiation available at the top of the atmosphere ($H_0$), reflects the quality of the day sunshine rate. Similar to Equation (10), it is expressed as follows:

$$K_{dt} = \frac{H_g}{H_0} \tag{44}$$

Figure 4 shows the daily distribution of the number of days versus the clearness index for Senia and Tlemcen sties.
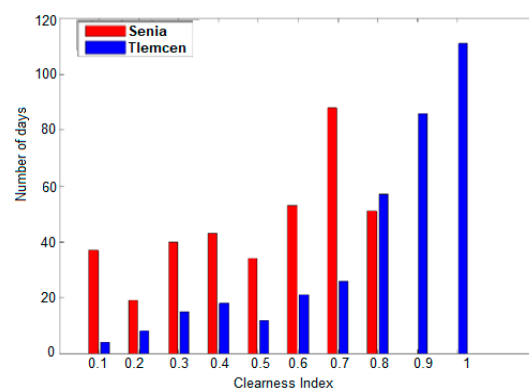


**Figure 4.** Daily distribution of the clearness index for Senia and Tlemcen.

The number of days, which have a high clearness index (from 0.9 to 1) is higher for Tlemcen site than Senia site where the majority of concerned periods are very sunny since 80% of the days have a clearness index greater than 0.6. This is not the case for the Senia where the number of days with clearness index within 0.6 to 0.7 is predominant at a percentage of 38% of the whole days. It can be explained by the fact that at Senia site, the change from a cloudy weather condition to sunny weather condition is less frequent, which characterizes a rapid and frequent degradation of the weather as shown in Figure 4. This is not the case for Tlemcen where the transition from cloudy weather condition to sunny weather condition is the most frequent, which characterizes a gradual improvement in the weather.

### 5.3. Annual Evolution of Daily Global Irradiations Measured on a Horizontal Plane

Figure 5 shows the comparison between three curves such as the daily extraterrestrial global solar irradiation in bleu, the measured daily global solar irradiation in brown, and the theoretical daily global solar irradiation under clear sky for both sites. It is worthy to note that the theoretical daily global solar irradiation under clear sky represents the daily global solar radiation that is available at the earth's surface for the considered locations in the absence of clouds.
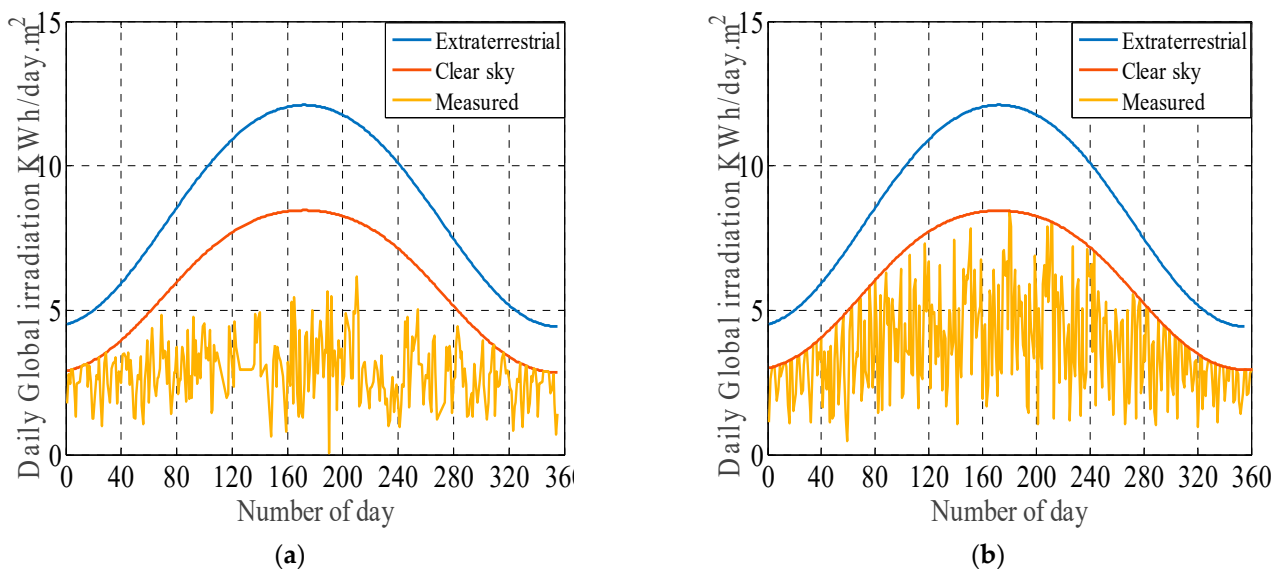
**(a)**

**(b)**

**Figure 5.** The annual evolution of the daily global solar irradiations on a horizontal plane; the measured (brown), the theoretical (red, and the extraterrestrial (bleu). (**a**) The Tlemcen site; (**b**) the Senia site.

All the curves are representing the north-west of the country. Their analysis indicates that the daily global solar irradiation values are maximum in winter and minimum in summer in considered sites. However, the daily solar irradiation values obtained in summer for Tlemcen are higher than those obtained for Senia. At this same period, the daily global solar irradiation can reach 8.4 KWh in Tlemcen site, while it does not exceed 6.15 KWh in Senia site.

### 5.4. Histograms of Annual Change in Monthly Global Irradiations for Both Sites

Figure 6 shows the monthly cumulative global solar irradiation for Senia and Tlemcen sites. For Tlemcen, it is observed that the important proportion of the high global solar irradiation is in the period between March and September (greater than 200 KWh). In the period between October and January, there is a remarkable decrease in the received global solar irradiation (less than 176 KWh), which relates to days with heavy cloud cover. On the other side, the global solar irradiation varies very rapidly around the spring equinox and around the winter solstice, and it varies slightly around autumn equinox and summer solstice. It can be concluded that a very high global solar irradiation (297.16 KWh) is available in July and a very low global solar irradiation (83.68 KWh) is available in January. For the site of Senia, it can be noticed that an important proportion of the high global solar irradiation is received only in July (219.82 KWh). Whereas, in the other months, there is a remarkable decrease in the received global solar irradiation (less than 159.59 KWh), which relates to days with important cloud cover. It can be deduced also that the global solar radiation varies very slowly around autumn and spring equinox as well as around winter solstice. This confirms the availability of a very high global solar irradiation (219.82 KWh) which is received in July and a very low global solar irradiation (43.39 KWh) which can be received in December.
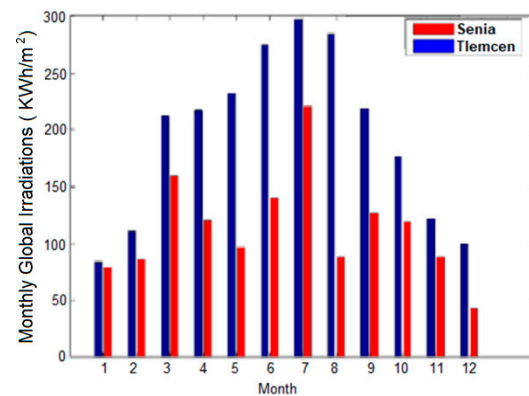
**Figure 6.** The distributions of the annual change of the monthly global solar irradiations measured on a horizontal plane for both sites.

*5.5. Histograms of Monthly Diffuses Irradiation Measured on Horizontal Plane for Both Sites*

　　　Figure 7 shows the monthly cumulative diffuse solar irradiation for Senia and Tlemcen. It can be clearly noted that the values for both sites are between 34 and 90 KWh for Tlemcen site, and between 34 and 70 KWh for Senia site. During the winter period, the diffuse solar irradiation are approximately reduced to the global solar irradiation, and during the summer period, the diffuse solar irradiations are much lower than the global solar irradiation for both sites.
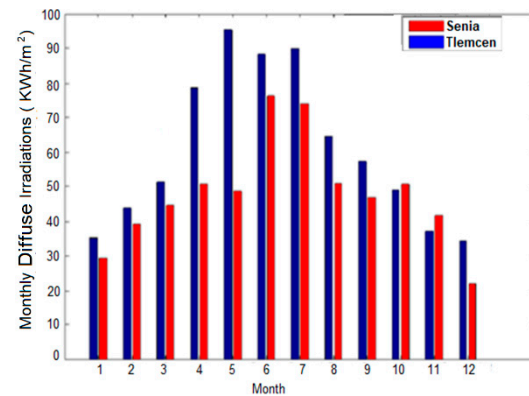


**Figure 7.** The distributions of the annual monthly average diffuse solar irradiation for both sites measured on a horizontal plane.

## 6. Validations Based on Previous Work in Literature

　　　This section focusses on the presentation of a comparative study based on the obtained global and diffuse solar radiations from the Capderou and R.Sun models, and the experimental measurements based on the data collected onsite under clear sky. This comparison has been carried out within four specific days on both studied sites.

*6.1. Validation Based on Capderou and R.Sun Models*

6.1.1. Results Obtained on the Site of Senia

Global Solar Radiations

　　　Figure 8 presents the global solar radiation estimated by the Capderou and R.Sun models, and the collected measurements on the site of Senia, which were carried out based on the incident solar radiation on a horizontal plane where four days under clear skies are selected from different seasons to achieve this study.
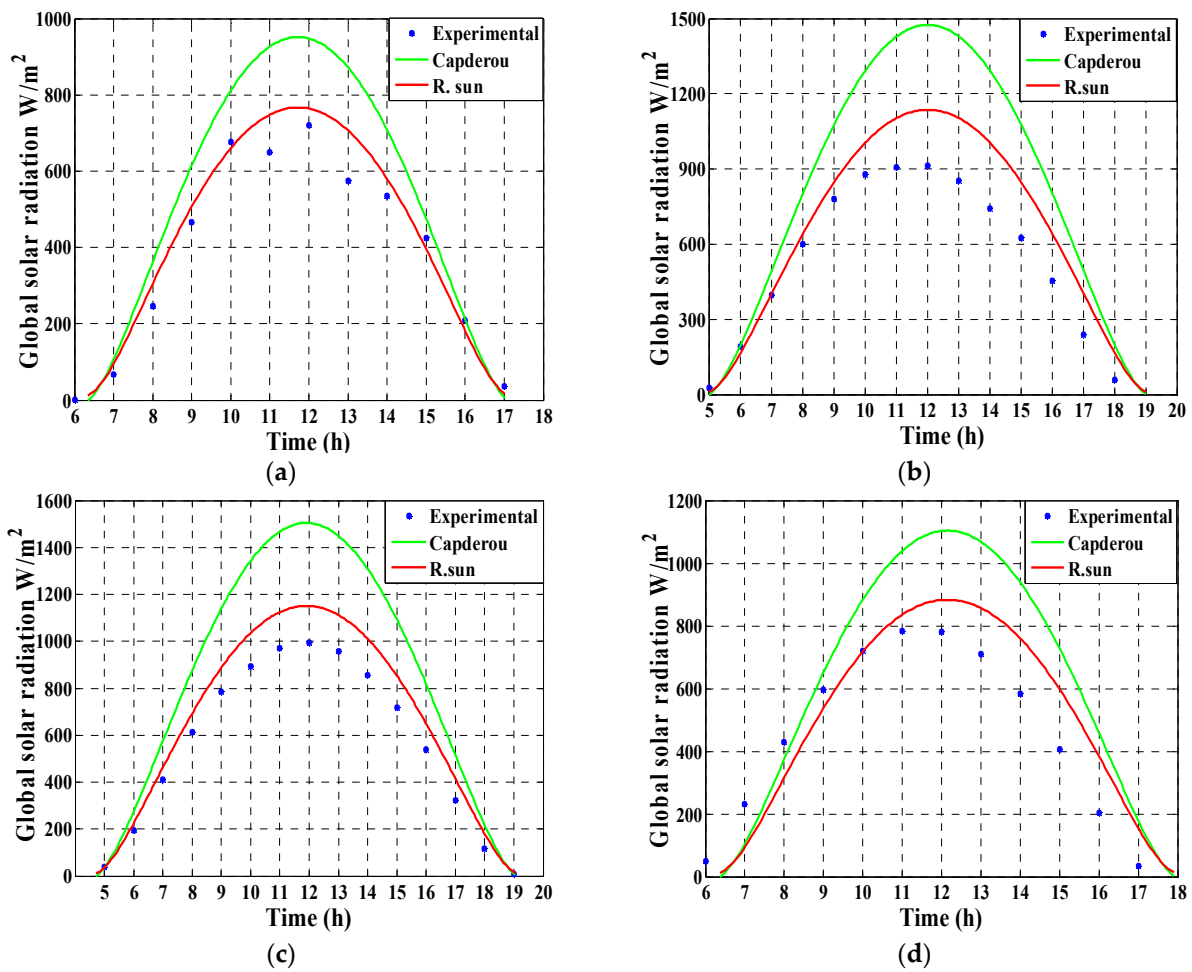
**Figure 8.** The comparison between the measured global solar radiations and the global solar radiation obtained by Capderou and R.Sun models for the site of Senia. (**a**)16 February 2006; (**b**) 20 May 2006; (**c**) 1 July 2006; (**d**) 2 October 2006.

Diffuse Solar Radiations

Figure 9 presents the diffuse solar radiation estimated by the Capderou and R.Sun models, and the collected measurements on the site of Senia, where four days under clear skies are selected from different seasons to achieve this study.
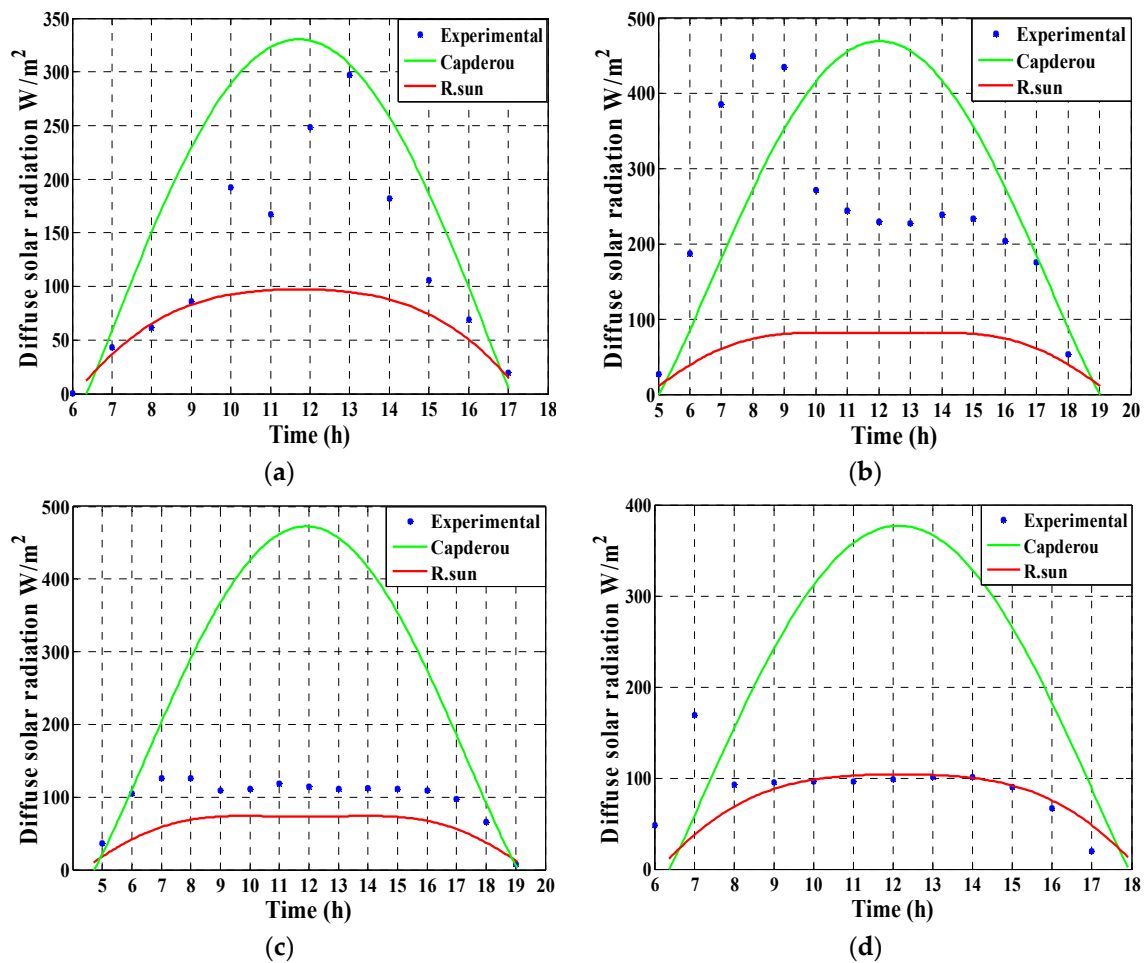
**Figure 9.** The comparison between the measured diffuse solar radiations and the diffuse solar radiation obtained by Capderou and R.Sun models for the site of Senia. (**a**) 16 February 2006; (**b**) 20 May 2006; (**c**) 1 July 2006; (**d**) 2 October 2006.

6.1.2. Results Obtained on the Site of Tlemcen

Global Solar Radiations

Figure 10 presents the global solar radiation estimated by the Capderou and R.Sun models, and the collected measurements on the site of Tlemcen, which were carried out based on the incident solar radiation on a horizontal plane where four days under clear skies are selected from different seasons to carry out the study.

Diffuse Solar Radiations

Figure 11 presents the diffuse solar radiation estimated by the Capderou and R.Sun models, and the collected measurements on the site of Tlemcen, where four days under clear skies are selected from different seasons to achieve this study.

6.1.3. Discussion and Interpretations

Based on the aforementioned results, it can be said that the Capderou model gives an overestimation of the global and diffuse components of the solar radiation for both sites. However, only less difference concerning the global solar radiation is observed in the case of the Tlemcen site. On the other side, the R.Sun model overestimates the global solar radiation for Senia site and underestimates the same component for the Tlemcen site. However, the difference resulting from the application of the Capderou model has led to a remarkable influence on the estimation of the global solar radiation for the Tlemcen site, whereas the difference resulting from the application of the R.Sun model has led to a limited influence. It can be noticed also that the R.Sun model ensures a good estimation

of the diffusion component than the Capderou model for both sites. Indeed, based on the analysis of the equations calculating the diffuse solar radiations from the two models, it is found that they have the same shape and they are function of the same input variables such as $m_a$ (air mass) and $\delta_R$ (integral Rayleigh optical thickness). While the R.Sun model uses improved formulas to calculate these variables, which gives improved precision of the calculations. However, R.Sun model leads to better estimation of the global and diffuse solar radiations in summer and autumn compared to winter and spring months. It can be noticed also that both models perform well at sunrise and sunset regarding global solar radiation but they diverge from each other in the middle of the day where the difference is maximum at noon.

*6.2. Validation of the Proposed Model Based on the Monthly Averages Results of the Global Solar Irradiation Obtained Experimentally and by the Coppolino Model*

6.2.1. The Monthly Averages Results of the Global Solar Irradiation for Both Sites

Tables 6 and 7 present the comparison of the monthly averaged global solar irradiations obtained at the Senia and Tlemcen sites respectively, based on the experimental measurements, the Coppolino model [34,35], and the proposed model in this paper.
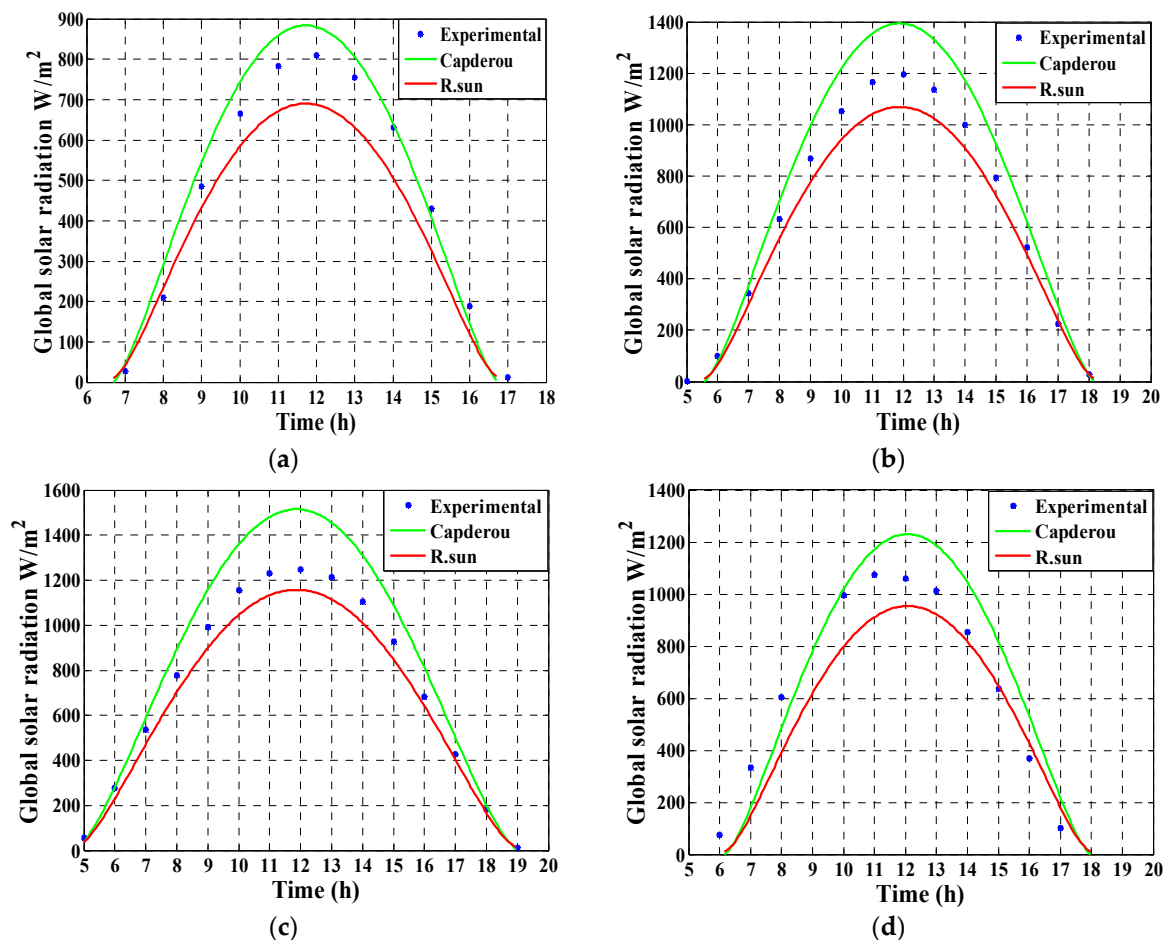


**Figure 10.** The comparison between the measured global solar radiations and the global solar radiation obtained by Capderou and R.Sun models for the site of Tlemcen. (**a**) 22 January 2006; (**b**) 8 April 2006; (**c**) 29 June 2006; (**d**) 26 September 2006.
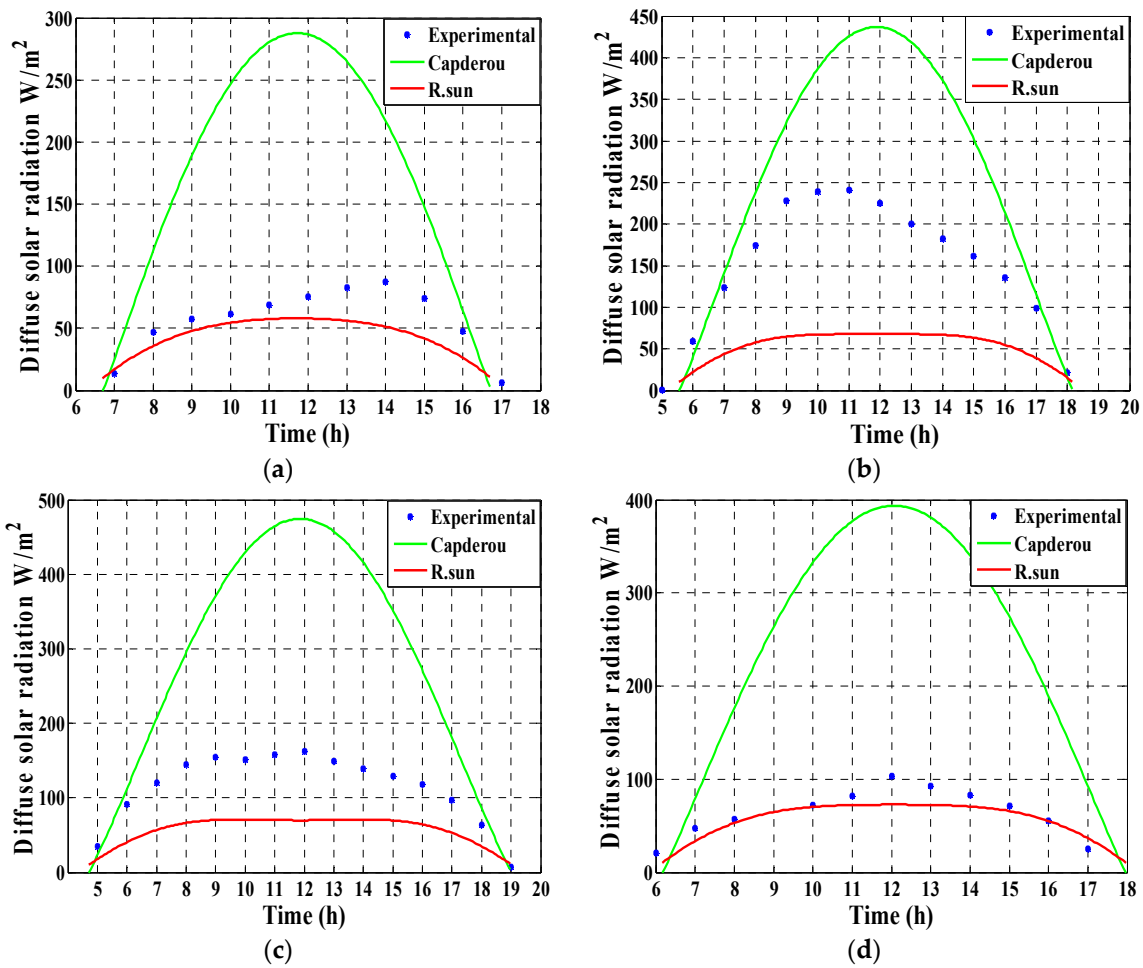
**Figure 11.** The comparison between the measured diffuse solar radiations and the diffuse solar radiation obtained by Capderou and R.Sun models for the site of Tlemcen. (**a**) 22 January 2006; (**b**) 8 April 2006; (**c**) 29 June 2006; (**d**) 26 September 2006.

**Table 6.** The results for Senia site (MJ/m²/Jour).

| Month | Experimental | Proposed Model | $E_{r1}\%$ | Coppolino Model | $E_{r2}\%$ |
|---|---|---|---|---|---|
| January | 9.1114 | 9.1660 | 0.5997 | 8.2871 | 8.9927 |
| February | 11.0130 | 11.0563 | 0.3926 | 11.9424 | 8.4059 |
| March | 18.1234 | 18.5384 | 2.2898 | 11.9424 | 8.4059 |
| April | 19.2266 | 19.2905 | 0.3323 | 16.6103 | 19.2706 |
| May | 19.4342 | 19.5692 | 0.6948 | 13.4004 | 30.8333 |
| June | 18.0808 | 18.0808 | 0.0000 | 17.3143 | 4.2392 |
| July | 25.5268 | 25.5565 | 0.1164 | 18.7369 | 26.5680 |
| August | 10.1663 | 10.1019 | 0.6335 | 15.0157 | 48.0037 |
| September | 17.5243 | 17.4682 | 0.3206 | 15.9186 | 9.1922 |
| October | 13.6263 | 13.6527 | 0.1941 | 12.5596 | 7.8132 |
| November | 10.3746 | 10.6091 | 2.2606 | 10.8900 | 4.8578 |
| December | 7.4383 | 7.4201 | 7.4201 | 1.2059 | 83.9933 |
| **Annual Mean** | **14.9705** | **15.0425** | **0.4807** | **13.0360** | **12.9220** |

**Table 7.** The results for Tlemcen site (MJ/m$^2$/Jour).

| Month | Experimental | Proposed Model | $E_{r1}$% | Coppolino Model | $E_{r2}$% |
|---|---|---|---|---|---|
| January | 10.7582 | 10.8067 | 0.4505 | 8.4171 | 21.6636 |
| February | 14.1571 | 14.2167 | 0.4210 | 10.2529 | 27.4620 |
| March | 24.5698 | 24.6340 | 0.2613 | 14.6149 | 40.4113 |
| April | 25.9839 | 26.0739 | 0.3464 | 20.2534 | 21.9777 |
| May | 27.0138 | 26.9943 | 0.0723 | 19.0394 | 29.5411 |
| June | 33.0110 | 33.0197 | 0.0264 | 21.1020 | 36.0665 |
| July | 34.0701 | 34.5203 | 0.4370 | 23.8638 | 30.4351 |
| August | 32.7533 | 33.0826 | 1.0053 | 22.8061 | 30.0678 |
| September | 25.9843 | 26.2232 | 0.9196 | 18.5853 | 28.2222 |
| October | 20.0092 | 20.3003 | 1.4548 | 14.1162 | 29.0292 |
| November | 14.5769 | 14.7367 | 1.0965 | 11.1648 | 23.1540 |
| December | 11.4754 | 11.5699 | 0.8235 | 5.6641 | 50.2280 |
| **Annual Mean** | **22.8885** | **23.0148** | **0.5516** | **15.8231** | **30.6882** |

6.2.2. Discussion and Interpretations

For the site of Senia, the obtained results in Table 6 show that Coppolino model predicts the annual averaged daily global solar irradiation with good reliability. Regarding the monthly average of the global solar irradiation, the months of May, July, August, December present a very important relative error as presented in Table 6, at this level the model overestimates the monthly solar irradiation, this is probably due to the meteorological conditions of the year 2006 in the site of the present study. For the site of Tlemcen, the relative error is practically very large for all the months of the year as presented in Table 7, this is probably due to the elevation of Tlemcen (843 m). It can be said that this model cannot ensure the prediction with good reliability and precision in the site located beyond a certain elevation, furthermore the model does not take into account other parameters, as, Linke turbidity factor. In contract, the proposed model can ensure the best estimation or prediction in both sides compared to the Coppolino model as it can be clearly confirmed from the results presented in Tables 6 and 7. It is obvious, that the relative error $E_{r1}$ is practically neglected in case of the proposed model compared to the Coppolino model and in the same time this relative error is very small which confirms that the prediction is very performant when the monthly average values are used. It can be concluded from this results that the proposed model overcome the main deficiencies and drawbacks met with Coppolino model in both sites.

*6.3. Validation of the Proposed Model Based on the Obtained Daily Cummulative Global Solar Irradiation under Clear Sky from the Experimental and the Mefti Model (1996)*

6.3.1. The Daily Accumulative Results under Clear Sky for Both Sites

Tables 8 and 9 present the comparison of the global solar irradiations obtained at the Senia and Tlemcen sites respectively, based on the experimental measurements, the Mefti model [3], and the proposed model in this paper.

**Table 8.** Results for Senia site (KWh/m$^2$).

| Date Under Clear Sky | Experimental | Proposed Model | $E_{r1}$% | Mefti Model | $E_{r2}$% |
|---|---|---|---|---|---|
| 16 February | 4.61 | 4.52 | 1.95 | 4.4545 | 3.3734 |
| 20 May | 7.6664 | 7.97 | 3.81 | 7.7532 | 1.1328 |
| 1 July | 8.4192 | 8.65 | 2.85 | 7.9255 | 5.8636 |
| 2 October | 5.5308 | 6.22 | 4.75 | 5.8636 | 0.7042 |

**Table 9.** Results for Tlemcen site (KWh/m$^2$).

| Date Under Clear Sky | Experimental | Proposed Model | $E_{r1}$% | Mefti Model | $E_{r2}$% |
|---|---|---|---|---|---|
| 22 February | 4.9981 | 4.71 | 5.76 | 3.5192 | 29.5893 |
| 8 May | 9.0667 | 9.12 | 0.59 | 6.8388 | 24.5675 |
| 29 July | 10.8247 | 10.79 | 0.32 | 7.9681 | 26.3894 |
| 26 October | 7.1156 | 6.99 | 1.77 | 5.9400 | 16.5207 |

6.3.2. Discussion and Interpretation

From the obtained results, it can be clearly seen that the Mefti model predicts the daily average of the global solar irradiation under clear skies with very good accuracy on the Senia site. However, this is not the case for the Tlemcen site. Whereas it is obvious that the resulting difference is very important, probably due to the model which is based on a statistical study to extract the maximum global solar irradiation received during the decade 1972–1982 in the regions where the study has been carried out. However, for the proposed model it works better than Mefti model where the absolute relative error $E_{r1}$ is very small less than 5.8 for the sites of Tlemcen and Senia respectively, compared with the relative error obtained by Mefti model $E_{r2}$ which is greater than 16.5 for the site of Tlemcen as presented in Tables 8 and 9 respectively. These results clearly confirm the advantage of the proposed models in both sites in the case of daily prediction of the days under clear sky.

*6.4. Validation of the Proposed Model Based on the Obtained Daily Cummulative Global Solar Irradiation under Clear Sky from the Experimental and Sivkov Model (1964)*

6.4.1. The Monthly Cumulative Results of the Global Solar Irradiation Obtained Experimentally and Based on the Sivkov Model

Tables 10 and 11 present the comparison of the global solar irradiations obtained at the Senia and Tlemcen sites respectively, based on the experimental measurements, the Sivkov model [36], and the proposed model in this paper.

**Table 10.** The results for Senia site (MJ/m$^2$).

| Date by Clear Sky | Experimental | Proposed Model | $E_{r1}$% | Sivkov Model | $E_{r2}$% |
|---|---|---|---|---|---|
| January | 282.4536 | 281.52 | 0.33 | 265.1043 | 6.1424 |
| February | 308.3654 | 307.28 | 0.35 | 319.0375 | 3.4609 |
| March | 561.8252 | 550.99 | 1.93 | 553.3256 | 1.5129 |
| April | 422.9844 | 410.01 | 3.07 | 517.8925 | 22.4377 |
| May | 349.8155 | 320.54 | 8.37 | 522.2069 | 30.8333 |
| June | 506.2628 | 499.57 | 1.32 | 622.7134 | 49.2806 |
| July | 791.3303 | 780.11 | 1.42 | 824.0640 | 23.0020 |
| August | 315.1566 | 300.02 | 4.80 | 585.2954 | 48.0037 |
| September | 455.6330 | 522.82 | 14.75 | 502.0081 | 4.1365 |
| October | 422.4143 | 411.97 | 2.47 | 452.2510 | 7.0634 |
| November | 311.2382 | 301.19 | 3.23 | 319.5519 | 2.6712 |
| December | 156.2049 | 171.92 | 10.06 | 176.8331 | 13.2059 |
| **Annual Cumulative** | **4883.6842** | **4857.94** | **0.53** | **5660.2837** | **15.9019** |

**Table 11.** The results for Tlemcen (MJ/m$^2$).

| Date by Clear Sky | Experimental | Proposed Model | $E_{r1}$% | Sivkov Model | $E_{r2}$% |
|---|---|---|---|---|---|
| January | 301.2310 | 288.23 | 4.32 | 256.0410 | 15.0018 |
| February | 396.4000 | 381.12 | 3.85 | 341.4205 | 13.8697 |
| March | 761.6642 | 735.01 | 3.5 | 600.1289 | 21.2082 |
| April | 779.5162 | 763.18 | 2.1 | 660.2086 | 15.3053 |
| May | 837.4283 | 800.14 | 4.45 | 689.6181 | 17.65.05 |
| June | 990.3302 | 955.99 | 3.47 | 833.3348 | 15.8528 |
| July | 1065.500 | 1005.09 | 5.67 | 889.2017 | 16.5440 |
| August | 1015.400 | 1002.13 | 1.31 | 857.7873 | 15.5183 |
| September | 779.5284 | 719.19 | 7.74 | 646.1216 | 17.1138 |
| October | 620.2838 | 588.29 | 5.16 | 520.6633 | 16.0605 |
| November | 437.3076 | 398.37 | 8.9 | 377.9954 | 13.5630 |
| December | 358.6669 | 329.30 | 8.19 | 308.4884 | 13.2822 |
| **Annual Cumulative** | **8343.2564** | **7966.04** | **4.52** | **6981.0096** | **16.33** |

### 6.4.2. Discussion and Interpretations

For the site of Senia as presented in Table 10, the examination of the obtained results show that the values of global monthly cumulative solar radiation (G) estimated by Sivkov model are quite close to the experimental values in summer and autumn seasons. However, the relative differences are very remarkable, they oscillate between 20 and 50% from April to June, and becomes 85% in August. On the other side, for the site of Tlemcen the relative difference is practically important around the year as presented in Table 11. It should be noted that Sivkov model overestimates the monthly cumulative of the global solar irradiation for Senia site and underestimates it for Tlemcen site. This is probably due to the meteorological conditions of 2006 year. In general, and through the obtained results, it can be said that the Sivkov model can be used for the sites of Senia and Tlemcen to predict the monthly global solar irradiation, especially if other operating parameter are taken into account and the data collected on site cover a greater number of years such as from 3 to 5 years. However, the results obtained on the proposed model in this paper show the important advantages for the prediction of the cumulative solar irradiation in both sites compared to the Sivkov model. Indeed, the relative error calculated for the proposed model $E_{r1}$ is practically neglected in front of the relative error calculated, $E_{r2}$, based on the results obtained from the Sivkov model. On the other side, the proposed model allows the predication of the monthly cumulative solar irradiation with better performances. In the same time the disadvantages faced in the Sivkov model are not presented in the proposed model which confirms the validity of the proposed model under different weather conditions and the differences of the geographic locations.

### 6.5. Discussions on the Overall Obtained Results

Based on the overall obtained result it can be said that the R.Sun model was more favorable than Capderou model regarding estimation of global and diffuse solar radiations for both sites. However, concerning estimation of monthly average per day of the horizontal global irradiation, Coppolino model seems more accurate. While for the estimation of the monthly cumulative of global solar radiation, Sivkov model is more favorable. The daily average of horizontal global irradiation per clear sky using the Mefti model, the results seem more favorable for site of Senia than site of Tlemcen. Simulation results show that R.Sun model is generally the most favorable for estimating incident solar radiation on a horizontal sensor, even if the diffuse solar radiation estimated by it, sometimes presents a significant difference versus the experimental diffuse solar radiation. Moreover, the R.Sun model overestimates global irradiation for Senia and underestimates it for Tlemcen. On the other hand, Capderou model overestimates all the components of the radiation for both sites and sometimes gives results that diverge with values measured at both sites. However,

it is noticed that this model performs well at sunrise and sunset, whereas R.Sun model is the most recommended outside of this range. For the estimation of the monthly average per day of the Global radiation incident on a horizontal sensor, the Coppolino model is more consistent for the site of Senia than for the site of Tlemcen. Therefore, according to the relative errors found for the Site of Senia, this model is very reliable especially during the months of: January, February, June, September, October, and November. December has a very large relative error probably due to the weather conditions during this month. For the site of Tlemcen, the relative error is practically constant and is quite high during every month. In addition, the studies carried out on both sites prove that Sivkov model gives the best estimates concerning the monthly total of global irradiation for Senia than Tlemcen. For the site of Senia, Sivkov model is very efficient except for the months of May and August where the relative error is very large, but which has little influence on the annual average. On the other hand, for site of Tlemcen, the error is practically constant and oscillates around 16%. The Mefti model allows predicting the daily average of the global irradiation per clear sky with very good reliability for site of Senia, but does not deal with the altitude problem, which makes it less reliable for the site of Tlemcen. However, the obtained results of the estimation of all the aforementioned components using the proposed model in this paper show that it can be suitable for almost all the cases. Indeed, the proposed model gains the advantages of the previously presented models in the literature and in the same it overcomes the drawbacks related to the occurred changes when moving from one site to another due to the location characteristics or climatic conditions and other parameters influencing the measurement quality. Furthermore, the proposed model is found to be more accurate compared to the real data collected onsite which is explained by the less relative errors ($E_{r1}$) obtained in all the cases as presented in Tables 6–11. Another important advantage of the proposed model is validity for the estimation or prediction of solar irradiation for different periods of prediction such as for the day, month, and annually, and the same for the kind of the estimated data such as cumulative or averaged values.

## 7. Conclusions

The present paper focusses on the development of a solar potential prediction model based on real data measurements of the solar radiation collected from two existing radiometric stations installed in two selected sites in Algeria such as the Tlemcen site and the Senia sites. These two sites were selected for the validation of the developed model due to their weather conditions and elevations differences. Indeed, the proposed model presents a simple linear relation with easy implementation which can be built based on the combination of two linear correlations related to the ratio of the daily diffuse solar irradiation to the daily global solar irradiation. The first correlation is function of the sunshine fraction and the second correlation is function of the clearness index. On the other side, of the validation of the proposed model, it was mandatory to check its applicability compared with previously developed models in the literature. Based on the results obtained in this paper, it can be concluded that the proposed model can be a promising tool for the prediction and estimation of the solar components such as radiation and irradiation and at the same time covers all the regions with different climatic conditions and geographic discrepancies, which cannot be achieved with all the proposed models up to date. On the other side, the proposed model can be an effective tool for the designers of the solar power plant of all kinds in any regions under any weather conditions such as photovoltaic, thermal, and concentrated solar based. Finally, it can be said that the proposed model can be used for the evaluation of the solar potential in any region in the world based on the collected meteorological data on site.

## References

1. Fekkak, B.; Menaa, M.; Boussahoua, B. Control of transformerless grid-connected PV system using average models of power electronics converters with MATLAB/Simulink. *Sol. Energy* **2018**, *173*, 804–813. [CrossRef]
2. Capderou, M. *Atlas Solaire de L'algerie: Aspect Energétique*; Tome 1; Office des Publications Universitaires: Algiers, Algeria, 1985; Volumes 1–2.
3. Mefti, A. Contribution à la Détermination du Gisement Solaire par Traitement de Données Solaires au sol et D'images Météosat. Ph.D. Thesis, University of Science and Technology Houari Boumediene, Bab Ezzouar, Algiers, 2007.
4. Qu, Z. La Nouvelle Méthode Heliosat-4 Pour L'évaluation du Rayonnement Solaire au Sol. Ph.D. Thesis, Ecole Nationale Supérieure des Mines de Paris, Paris, France, 2013.
5. Fariza, M. Détermination du Gisement Solaire par Traitement D'images MSG. Master's Thesis, Mouloud Maameri University of Tizi-Ouzou, Tizi Ouzou, Algiers, 2010.
6. Makade, R.G.; Chakrabarti, S.; Jamil, B. Prediction of global solar radiation using a single empirical model for diversified locations across India. *Urban Clim.* **2019**, *29*, 100492. [CrossRef]
7. Perveen, G.; Rizwan, M.; Goel, N. Intelligent model for solar energy forecasting and its implementation for solar photovoltaic applications. *J. Renew. Sustain. Energy* **2018**, *10*, 063702. [CrossRef]
8. Da Silva, M.B.P.; Escobedo, J.F.; Rossi, T.J.; dos Santos, C.M.; da Silva, S.H.M.G. Performance of the Angstrom-Prescott Model (AP) and SVM and ANN techniques to estimate daily global solar irradiation in Botucatu/SP/Brazil. *J. Atmos. Sol.-Terr. Phys.* **2017**, *160*, 11–23. [CrossRef]
9. Beyazıt, N.I.; Ünal, F.; Bulut, H. Modeling of the hourly horizontal solar diffuse radiation in Sanliurfa, Turkey. *Therm. Sci.* **2020**, *24*, 939. [CrossRef]
10. Güçlü, Y.S.; Yeleğen, M.Ö.; Dabanlı, İ.; Şişman, E. Solar irradiation estimations and comparisons by ANFIS, Angström–Prescott and dependency models. *Sol. Energy* **2014**, *109*, 118–124. [CrossRef]
11. Muzathik, A.M.; Ibrahim, M.Z.; Samo, K.B.; Nik, W.W. Estimation of global solar irradiation on horizontal and inclined surfaces based on the horizontal measurements. *Energy* **2011**, *36*, 812–818. [CrossRef]
12. Mubiru, J. Using artificial neural networks to predict direct solar irradiation. *Adv. Artif. Neural Syst.* **2011**, *2011*, 142054. [CrossRef]
13. Medeiros, F.J.D.; Silva, C.M.; Bezerra, B.G. Calibration of ångström-Prescott equation to estimate daily solar radiation on Rio Grande do Norte state, Brazil. *Rev. Bras. Meteorol.* **2017**, *32*, 409–416. [CrossRef]
14. Dervishi, S.; Mahdavi, A. Computing diffuse fraction of global horizontal solar radiation: A model comparison. *Sol. Energy* **2012**, *86*, 1796–1802. [CrossRef]
15. Li, F.; Zhong, L.; Cheung, S.G.; Wong, Y.; Shin, P.; Lei, A.; Zhou, H.; Song, X.; Tam, N. Is Laguncularia racemosa more invasive than Sonneratia apetala in northern Fujian, China in terms of leaf energetic cost? *Mar. Pollut. Bull.* **2020**, *152*, 110897. [CrossRef] [PubMed]
16. Hofierka, J.; Suri, M. The solar radiation model for Open source GIS: Implementation and applications. In Proceedings of the Open Source GIS-GRASS Users Conference, Trento, Italy, 11–13 September 2002; Volume 2002, pp. 51–70.
17. Badescu, V.; Gueymard, C.A.; Cheval, S.; Oprea, C.; Baciu, M.; Dumitrescu, A.; Iacobescu, F.; Milos, I.; Rada, C. Accuracy and sensitivity analysis for 54 models of computing hourly diffuse solar irradiation on clear sky. *Theor. Appl. Clim.* **2013**, *111*, 379–399. [CrossRef]
18. Dogniaux, R. *Representation Analytique des Composantes du Rayonnement Solaire*; Serie A No. 83; The Royal Meteorological Institute of Belgium: Brussels, Belgium, 1974.
19. López, G.; Batlles, F.J. Estimate of the atmospheric turbidity from three broad-band solar radiation algorithms. A comparative study. *Ann. Geophys. Eur. Geosci. Union* **2004**, *22*, 2657–2668. [CrossRef]

20. Klimenta, D.; Lekic, J.; Arsic, S.; Tasic, D.; Krstic, N.; Radosavljevic, D. A Novel Procedure for Quick Design of Off-Grid PV Water Pumping Systems for Irrigation. *Elektron. Elektrotechnika* **2021**, *27*, 64–77. [CrossRef]

21. Mahjoubi, A. Global Solar Radiation in Two Tunisian Cities: Comparison of Prediction and Measured Data. *J. Sustain. Energy* **2018**, *4*, 101–109.

22. Marif, Y.; Chiba, Y.; Belhadj, M.M.; Zerrouki, M.; Benhammou, M. A clear sky irradiation assessment using a modified Algerian solar atlas model in Adrar city. *Energy Rep.* **2018**, *4*, 84–90. [CrossRef]

23. Abdeladim, K.; Razagui, A.; Semaoui, S.; Arab, A.H. Updating Algerian solar atlas using MEERA-2 data source. *Energy Rep.* **2020**, *6*, 281–287. [CrossRef]

24. Flores, J.L.; Karam, H.A.; Marques Filho, E.P.; Pereira Filho, A.J. Estimation of atmospheric turbidity and surface Radiative parameters using broadband clear sky solar irradiance models in Rio de Janeiro-Brasil. *Theor. Appl. Climatol.* **2016**, *123*, 593–617. [CrossRef]

25. Chabane, F.; Guellai, F.; Michraoui, M.Y.; Bensahal, D.; Bima, A.; Moummi, N. Prediction of the global solar radiation onnclined area. *Appl. Sol. Energy* **2019**, *55*, 41–47. [CrossRef]

26. Gougui, A.; Djafour, A.; Khelfaoui, N.; Boutelli, H. Empirical models validation to estimate global solar irradiance on a horizontal plan in Ouargla, Algeria. In *AIP Conference Proceedings*; AIP Publishing LLC: Melville, NY, USA, 2018; Volume 1968, p. 030045.

27. Ammar, R.B.; Ammar, M.B.; Oualha, A. Photovoltaic power forecast using empirical models and artificial intelligence approaches for water pumping systems. *Renew. Energy* **2020**, *153*, 1016–1028. [CrossRef]

28. Alam, F.; Rehman, S.U.; Rehman, S.; Jahangir, M.; Shoaib, M.; Siddiqui, I.; Ulfat, I. Empirical model development for the estimation of clearness index using meteorological parameters. *Turk. J. Electr. Eng. Comput. Sci.* **2019**, *27*, 4429–4441. [CrossRef]

29. Akinpelu, J.A.; Olawale, O.K.; Omole, O.T. Estimation of global solar radiation for Ikeja, Enugu and Kano, Nigeria. *J. Appl. Sci. Environ. Manag.* **2018**, *22*, 1877–1880. [CrossRef]

30. Smaili, K.; Merzouk, N.K.; Merzouk, M. Solar Climatic Atlas of Daily Usability by Variable Sky in Algeria. In Proceedings of the 2019 7th International Renewable and Sustainable Energy Conference (IRSEC), Agadir, Morocco, 27–30 November 2019; pp. 1–6.

31. Gairaa, K.; Benkaciali, S.; Guermoui, M. Clear-sky models evaluation of two sites over Algeria for PV forecasting purpose. *Eur. Phys. J. Plus* **2019**, *134*, 534. [CrossRef]

32. Geiger, M.; Diabaté, L.; Ménard, L.; Wald, L. Controlling the quality of solar irradiation data by means of a web service. In *European Geophysical Society, 27th General Assembly*; European Geophysical Society: Munich, Germany, 2002; p. A-03419.

33. Kasten, F. The Linke turbidity factor based on improved values of the integral Rayleigh optical thickness. *Sol. Energy* **1996**, *56*, 239–244. [CrossRef]

34. Coppolino, S. Validation of a very simple model for computing global solar radiation in the European, African, Asian and North American areas. *Sol. Wind. Technol.* **1990**, *7*, 489–494. [CrossRef]

35. Coppolino, S. A very simple model for computing global solar radiation. *Sol. Wind Technol.* **1990**, *7*, 299–303. [CrossRef]

36. Sivkov, S.I. To the method of computing possible radiation in Italy. *Trans. Main. Geophys. Obs.* **1964**, *160*, 1–20.